

An Analysis of State Evolution for Approximate Message Passing with Side Information

Hangjin Liu
NC State University
Email: hliu25@ncsu.edu

Cynthia Rush
Columbia University
Email: cynthia.rush@columbia.edu

Dror Baron
NC State University
Email: barondror@ncsu.edu

Abstract—A common goal in many research areas is to reconstruct an unknown signal x from noisy linear measurements. Approximate message passing (AMP) is a class of low-complexity algorithms for efficiently solving such high-dimensional regression tasks. Often, it is the case that side information (SI) is available during reconstruction. For this reason a novel algorithmic framework that incorporates SI into AMP, referred to as approximate message passing with side information (AMP-SI), has been recently introduced. An attractive feature of AMP is that when the elements of the signal are exchangeable, the entries of the measurement matrix are independent and identically distributed (i.i.d.) Gaussian, and the denoiser applies the same non-linearity at each entry, the performance of AMP can be predicted accurately by a scalar iteration referred to as state evolution (SE). However, the AMP-SI framework uses different entry-wise scalar denoisers, based on the entry-wise level of the SI, and therefore is not supported by the standard AMP theory. In this work, we provide rigorous performance guarantees for AMP-SI when the input signal and SI are drawn i.i.d. according to some joint distribution subject to finite moment constraints. Moreover, we provide numerical examples to support the theory which demonstrate empirically that the SE can predict the AMP-SI mean square error accurately.

I. INTRODUCTION

High-dimensional linear regression is a well-studied model that has been used in many applications including compressed sensing [1], imaging [2], and machine learning and statistics [3]. The unknown signal $x \in \mathbb{R}^n$ is viewed through the linear model:

$$y = Ax + w, \quad (1)$$

where $y \in \mathbb{R}^m$ are the measurements, $A \in \mathbb{R}^{m \times n}$ is a known measurement matrix, and $w \in \mathbb{R}^m$ is measurement noise. The goal is to estimate the unknown signal x having knowledge only of the noisy measurements y and the measurement matrix A . When the problem is under-determined (i.e., $m < n$), in order for reconstruction to be successful, it is necessary to exploit structural or probabilistic characteristics of the input signal x . Often a prior distribution on the input signal x is assumed, and in this case approximate message passing (AMP) algorithms [1] can be used for the reconstruction task.

AMP [1], [4] is a class of low-complexity algorithms for efficiently solving high-dimensional regression tasks (1). AMP works by iteratively generating estimates of the unknown input vector, x , using a possibly non-linear denoiser function tailored to any prior knowledge about x . One favorable feature of AMP is that under some technical conditions on the measurement

matrix A and x , the observations at each iteration of the algorithm are almost surely equal in distribution to x plus independent and identically distributed (i.i.d.) Gaussian noise in the large system limit.

AMP with Side Information (AMP-SI): In information theory [5], when different communication systems share side information (SI), overall communication can become more efficient. Recently [6], [7], a novel algorithmic framework, referred to as AMP-SI, has been introduced for incorporating SI into AMP for high-dimensional regression tasks (1). AMP-SI has been empirically demonstrated to have good reconstruction quality and is easy to use. For example, we have proposed to use AMP-SI for channel estimation in emerging millimeter wave communication systems [8], where the time dynamics of the channel structure allow previous channel estimates to be used as SI when estimating the current channel structure [7].

We model each entry of the observed SI, denoted by $\tilde{x} \in \mathbb{R}^n$, as depending statistically on the corresponding entry of the unknown signal x through some joint probability density function (pdf), $f(X, \tilde{X})$. AMP-SI uses a conditional denoiser, $\eta_t : \mathbb{R}^2 \rightarrow \mathbb{R}$, to incorporate SI,

$$\eta_t(a, b) = \mathbb{E}[X | X + \lambda_t Z = a, \tilde{X} = b]. \quad (2)$$

The AMP-SI algorithm iteratively updates estimates of the input signal x : let $x^0 = 0$, the all-zeros vector, then

$$r^t = y - Ax^t + \frac{r^{t-1}}{\delta} \langle \eta'_{t-1}(x^{t-1} + A^T r^{t-1}, \tilde{x}) \rangle, \quad (3)$$

$$x^{t+1} = \eta_t(x^t + A^T r^t, \tilde{x}), \quad (4)$$

where $x^t \in \mathbb{R}^n$ is the estimate of input signal at iteration t , and the denoiser in (2) is applied entry-wise to vector inputs. The derivative $\eta'_t(s, \cdot) = \frac{\partial}{\partial s} \eta_t(s, \cdot)$ is with respect to the first input, and $\langle v \rangle$ is the empirical average of a vector v , i.e., $\langle v \rangle = \frac{1}{n} \sum_{i=1}^n v_i$. Using the denoiser in (2), the AMP-SI algorithm (3)-(4) provides the minimum mean squared error (MMSE) estimate of the signal when SI \tilde{X} is available [6].

State Evolution (SE): It has been proven that the performance of AMP, as measured, for example, by the normalized squared ℓ_2 -error $\frac{1}{n} \|x^t - x\|_2^2$ between the estimate x^t and true signal x , can be accurately predicted by a scalar recursion referred as SE [9], [10] when the measurement matrix A is i.i.d. Gaussian under various assumptions on the elements of the signal. The SE equation for AMP-SI is as follows. Assume

the entries of the noise w are i.i.d. $\sim f(W)$ with $\sigma_w^2 = \mathbb{E}[W^2]$, and let $\lambda_0 = \sigma_w^2 + \mathbb{E}[X^2]/\delta$. Then for $t \geq 0$,

$$\lambda_t^2 = \sigma_w^2 + \frac{1}{\delta} \mathbb{E} \left[\left(\eta_{t-1}(X + \lambda_{t-1}Z, \tilde{X}) - X \right)^2 \right], \quad (5)$$

where $(X, \tilde{X}) \sim f(X, \tilde{X})$ are independent of $Z \sim \mathcal{N}(0, 1)$, where we use $\mathcal{N}(\mu, \sigma^2)$ to denote a Gaussian distribution with mean μ and variance σ^2 .

Considering AMP-SI (3)-(4), however, we cannot directly apply the existing AMP theoretical results [9], [10], as the conditional denoiser (2) depends on the index i through the SI, meaning that different scalar denoisers will be used at different indices within the AMP-SI iterations. Recent results [11], however, extend the asymptotic SE analysis to a larger class of possible denoisers, allowing, for example, each element of the input to use a different non-linear denoiser as is the case in AMP-SI. We employ these results to rigorously relate the SE presented in (5) to the AMP-SI algorithm in (3)-(4).

Related Work: While integrating SI into reconstruction algorithms is not new, AMP-SI introduces a unified framework within AMP supporting arbitrary signal and SI dependencies. Prior work using SI has been either heuristic, limited to specific applications, or outside the AMP framework.

For example, Wang and Liang [12] integrate SI into AMP for a specific signal prior density, but the method is difficult to apply to other signal models. Ziniel and Schniter [13] develop an AMP-based reconstruction algorithm for a time-varying signal model based on Markov processes for the support and amplitude. This signal model is easily incorporated into the AMP-SI framework as discussed in the analysis of the birth-death-drift model of [6], [7]. Manoel et al. implement an AMP-based algorithm in which the input signal is repeatedly reconstructed in a streaming fashion, and information from past reconstruction attempts is aggregated into a prior, thus improving ongoing reconstruction results [14]. This reconstruction scheme resembles that of AMP-SI, in particular when the Bernoulli-Gaussian model is used (see Section II-B).

Contribution and Outline: Ma et al. use numerical experiments to show that SE (5) accurately tracks the performance of AMP-SI (3)-(4) [7], as was shown rigorously for standard AMP. Ma et al. conjecture that rigorous theoretical guarantees can be given for AMP-SI as well [7]. In this work, we analyze AMP-SI performance when the input signal and SI are drawn i.i.d. according to a general pdf $f(X, \tilde{X})$ obeying some finite moment conditions, the AMP-SI denoiser (2) is Lipschitz, and the measurement matrix A is i.i.d. Gaussian.

In Section II, we give the main results, examples for various signal and SI models, and numerical experiments comparing the empirical performance of AMP-SI and the SE predictions. The proof of our main theorem is provided in Section III.

II. MAIN RESULTS

A. Main Theorem

Our main result provides AMP-SI performance guarantees when considering *pseudo-Lipschitz* loss functions, which we define in the following.

Definition II.1. Pseudo-Lipschitz functions [9]: For $k \in \mathbb{N}_{>0}$ and any $n \in \mathbb{N}_{>0}$, a function $\phi : \mathbb{R}^n \rightarrow \mathbb{R}$ is *pseudo-Lipschitz of order k* if there exists a constant L , referred to as the pseudo-Lipschitz constant of ϕ , such that for any $x, y \in \mathbb{R}^n$,

$$|\phi(x) - \phi(y)| \leq L \left(1 + \frac{\|x\|^{k-1}}{\sqrt{n}} + \frac{\|y\|^{k-1}}{\sqrt{n}} \right) \frac{\|x - y\|}{\sqrt{n}}. \quad (6)$$

For $k = 1$, this definition coincides with the standard definition of a Lipschitz function. Throughout this work, $\|\cdot\|$ denotes the Euclidean norm.

We are now ready to state our main result. Throughout the paper we let $\stackrel{p}{\equiv}$ denote convergence in probability.

Theorem II.1. *For any order k pseudo-Lipschitz functions $\phi : \mathbb{R}^2 \rightarrow \mathbb{R}$ and $\psi : \mathbb{R}^3 \rightarrow \mathbb{R}$, assume the following.*

- (A1) *The measurement matrix A has i.i.d. Gaussian entries with mean 0 and variance $1/m$.*
- (A2) *The noise w is i.i.d. $\sim f(W)$ with finite $\mathbb{E}[|W|^k]$.*
- (A3) *The signal and SI (X, \tilde{X}) are sampled i.i.d. from $f(X, \tilde{X})$ with finite $\mathbb{E}[|X|^k]$, finite $\mathbb{E}[|\tilde{X}|^k]$, and finite $\mathbb{E}[|X\tilde{X}|]$.*
- (A4) *For $t \geq 0$, the denoisers $\eta_t(\cdot, \cdot)$ defined in (2) are Lipschitz continuous, meaning for scalars a_1, a_2, b_1, b_2 , and constant $L > 0$,*

$$|\eta_t(a_1, b_1) - \eta_t(a_2, b_2)| \leq L \|(a_1, b_1) - (a_2, b_2)\|.$$

Then,

$$\begin{aligned} \lim_m \frac{1}{m} \sum_{i=1}^m \phi(r_i^t, w_i) &\stackrel{p}{\equiv} \mathbb{E} \left[\phi(W + \sqrt{\lambda_t^2 - \sigma_w^2} Z_1, W) \right], \\ \lim_n \frac{1}{n} \sum_{i=1}^n \psi(x_i^t + [A^T r^t]_i, x_i, \tilde{x}_i) &\stackrel{p}{\equiv} \mathbb{E} \left[\psi(X + \lambda_t Z_2, X, \tilde{X}) \right], \end{aligned} \quad (7)$$

where Z_1, Z_2 are standard Gaussians, independent of $W \sim f(W)$ and $(X, \tilde{X}) \sim f(X, \tilde{X})$. In the above, x^t and r^t are defined in the AMP-SI recursion (3)-(4), and λ_t in the SE (5).

Section III contains the proof of Theorem II.1. The proof follows from Berthier *et al.* [11, Theorem 14] and the strong law of large numbers. The main technical details involve showing that our assumptions (A1)–(A4) are enough to satisfy the assumptions needed for [11, Theorem 14]. The details are given in Section III.

As a concrete example of how Theorem II.1 provides performance guarantees for AMP-SI, let us consider a few interesting pseudo-Lipschitz loss functions.

Corollary II.1.1. *Under assumptions (A1)–(A4), letting $\psi^1 : \mathbb{R}^3 \rightarrow \mathbb{R}$ be the ℓ_2 loss, $\psi^1(x, y, z) = (x - y)^2$, then by Theorem II.1,*

$$\lim_{n \rightarrow \infty} \frac{1}{n} \|x^t + A^T r^t - x\|^2 \stackrel{p}{\equiv} \lambda_t^2,$$

where λ_t^2 is defined in (5). Similarly if $\psi^2 : \mathbb{R}^3 \rightarrow \mathbb{R}$ is defined as $\psi^2(x, y, z) = (\eta_t(x, z) - y)^2$, then by Theorem II.1

$$\lim_{n \rightarrow \infty} \frac{1}{n} \|x^{t+1} - x\|^2 \stackrel{p}{\equiv} \delta(\lambda_t^2 - \sigma_w^2).$$

B. Examples

Next, we consider a few signal and SI models to show how one can derive the denoiser in (2), use this to construct the AMP-SI algorithm and the SE, and apply Theorem II.1. Before we get to the examples we state a lemma that allows us know about how functions with bounded derivative are Lipschitz.

Lemma II.2. *A function $\phi : \mathbb{R}^2 \rightarrow \mathbb{R}$ having bounded derivatives, $0 < D_1, D_2 < \infty$,*

$$\left| \frac{\partial}{\partial x} \phi(x, y) \right| \leq D_1 \quad \text{and} \quad \left| \frac{\partial}{\partial y} \phi(x, y) \right| \leq D_2$$

is Lipschitz continuous with Lipschitz constant $\sqrt{D_1^2 + D_2^2}$.

Proof. The result follows using the Triangle Inequality and Cauchy-Schwarz,

$$\begin{aligned} & |\phi(x_1, y_1) - \phi(x_2, y_2)| \\ &= |\phi(x_1, y_1) - \phi(x_1, y_2) + \phi(x_1, y_2) - \phi(x_2, y_2)| \\ &\leq |\phi(x_1, y_1) - \phi(x_1, y_2)| + |\phi(x_1, y_2) - \phi(x_2, y_2)| \\ &\leq D_2 |y_1 - y_2| + D_1 |x_1 - x_2| \\ &\leq \sqrt{D_2^2 + D_1^2} \sqrt{(y_1 - y_2)^2 + (x_1 - x_2)^2} \\ &= \sqrt{D_2^2 + D_1^2} \|(x_1, y_1) - (x_2, y_2)\|. \end{aligned} \quad (8)$$

□

1) *Gaussian-Gaussian Signal and SI:* In this model, referred to as the GG model henceforth, the signal has i.i.d. Gaussian entries with zero mean and finite variance and we have access to SI in the form of the signal with additive white Gaussian noise (AWGN). The signal, X , and SI, \tilde{X} , are related by

$$\tilde{X} = X + \mathcal{N}(0, \sigma^2 \mathbb{I}). \quad (9)$$

In this case, the AMP-SI denoiser (2) equals [7]

$$\begin{aligned} \eta_t(a, b) &= \mathbb{E} \left[X \mid X + \lambda_t Z = a, \tilde{X} = b \right] \\ &= \frac{\sigma_x^2 \sigma^2 a + \sigma_x^2 \lambda_t^2 b}{\sigma_x^2 (\sigma^2 + \lambda_t^2) + \sigma^2 \lambda_{t-1}^2}. \end{aligned} \quad (10)$$

Then the SE (5) can be computed as

$$\lambda_t^2 = \sigma_w^2 + \frac{1}{\delta} \left[\frac{\sigma_x^2 \sigma^2 \lambda_{t-1}^2}{\sigma_x^2 (\sigma^2 + \lambda_{t-1}^2) + \sigma^2 \lambda_{t-1}^2} \right]. \quad (11)$$

We note that the denoiser in (10) is Lipschitz continuous as a result of Lemma II.2 because

$$\left| \frac{\partial}{\partial a} \eta_t(a, b) \right| = \left| \frac{\sigma_x^2 \sigma^2}{\sigma_x^2 (\sigma^2 + \lambda_t^2) + \sigma^2 \lambda_{t-1}^2} \right| \leq 1,$$

and

$$\left| \frac{\partial}{\partial b} \eta_t(a, b) \right| = \left| \frac{\sigma_x^2 \lambda_t^2}{\sigma_x^2 (\sigma^2 + \lambda_t^2) + \sigma^2 \lambda_{t-1}^2} \right| \leq 1,$$

and therefore the assumptions **(A1) – (A5)** are satisfied in the GG case and we can apply Theorem II.1.

2) *Bernoulli-Gaussian Signal and SI:* The Bernoulli-Gaussian (BG) model reflects scenario in which one wishes to recover a sparse signal and has access to SI in the form of the signal with AWGN as in (9). In this model, each entry of the signal is independently generated according to $x_i \sim \epsilon \mathcal{N}(0, 1) + (1 - \epsilon) \delta_0$, where δ_0 is the Dirac delta function at 0. In words, the entries of the signal independently take the value 0 with probability $1 - \epsilon$ and are $\mathcal{N}(0, 1)$ with probability ϵ . In this case, the AMP-SI denoiser (2) equals [7]

$$\begin{aligned} \eta_t(a, b) &= \mathbb{E} \left[X \mid X + \lambda_t Z = a, \tilde{X} = b \right] \\ &= \Pr(X \neq 0 | a, b) \mathbb{E} [X | a, b, X \neq 0] \\ &= \Pr(X \neq 0 | a, b) \frac{\sigma^2 a + \lambda_t^2 b}{\sigma^2 + \lambda_t^2 + \sigma^2 \lambda_t^2}, \end{aligned} \quad (12)$$

where, letting $\rho_{\tau^2}(x)$ be the zero-mean Gaussian density with variance τ^2 evaluated at x , and defining $\nu_t := \sigma^2 \lambda_t^2 (\sigma^2 + \lambda_t^2 + \sigma^2 \lambda_t^2)$,

$$\Pr(X \neq 0 | a, b) = (1 + T_{a,b})^{-1}, \quad (13)$$

where we denote

$$\begin{aligned} T_{a,b} &:= \frac{(1 - \epsilon) \rho_{\lambda_t^2}(a) \rho_{\sigma^2}(b)}{\epsilon \rho_{1 + \sigma^2}(b) \rho_{\frac{\sigma^2}{1 + \sigma^2} + \lambda_t^2} \left(\frac{b}{1 + \sigma^2} - a \right)} \\ &= \left(\frac{1 - \epsilon}{\epsilon} \right) \sqrt{\frac{\sigma^2 + \lambda_t^2 + \sigma^2 \lambda_t^2}{\lambda_t^2 \sigma^2}} \\ &\quad \exp \left\{ \frac{-(\sigma^2 a + \lambda_{t-1}^2 b)^2}{2 \sigma^2 \lambda_{t-1}^2 (\sigma^2 + \lambda_t^2 + \sigma^2 \lambda_t^2)} \right\} \\ &= \left(\frac{1 - \epsilon}{\epsilon} \right) \frac{\nu_t \sqrt{2\pi}}{\lambda_t^2 \sigma^2} \rho_{\nu_t}(\sigma^2 a + \lambda_t^2 b), \end{aligned} \quad (14)$$

Then the SE (5) can be computed as

$$\lambda_t^2 = \sigma_w^2 + \frac{1}{\delta} \left(\frac{T_{a,b}}{1 + T_{a,b}} \right)^2 \left[\frac{(\sigma^2 + \lambda_{t-1}^2) + \sigma^2 \lambda_{t-1}^2}{\sigma^2 + \lambda_{t-1}^2 + \sigma^2 \lambda_{t-1}^2} \right]. \quad (15)$$

We again use Lemma II.2 to show that the denoiser defined in (12) and (13) is Lipschitz continuous so that the assumptions **(A1) – (A5)** are satisfied in the BG case and we can apply Theorem II.1. We study the partial derivatives. Denote

$$f_{a,b} := \frac{\sigma^2 a + \lambda_t^2 b}{\sigma^2 + \lambda_t^2 + \sigma^2 \lambda_t^2}. \quad (16)$$

Combining (13) and (14) and (16),

$$\eta_t(a, b) = (1 + T_{a,b})^{-1} f_{a,b}.$$

Then,

$$\begin{aligned} & \left| \frac{\partial \eta_t(a, b)}{\partial a} \right| \\ &= \left| \frac{1}{1 + T_{a,b}} \left[\frac{\partial f_{a,b}}{\partial a} \right] - \frac{1}{(1 + T_{a,b})^2} \left[\frac{\partial T_{a,b}}{\partial a} \right] f_{a,b} \right| \\ &\leq \frac{(1 + 2T_{a,b})}{(1 + T_{a,b})^2} \left| \frac{\partial f_{a,b}}{\partial a} \right| + \frac{1}{(1 + T_{a,b})^2} \left| \frac{\partial (T_{a,b} f_{a,b})}{\partial a} \right|. \end{aligned} \quad (17)$$

Now we show upperbounds for the two terms of (17) separately. For the first term, we see that $\frac{\partial f_{a,b}}{\partial a} \leq 1$, so

$$\frac{(1 + 2T_{a,b})}{(1 + T_{a,b})^2} \left| \frac{\partial f_{a,b}}{\partial a} \right| \leq 1.$$

Now we consider the second term of

Consider the second term of (17). First we note that

$$\frac{1}{(1 + T_{a,b})^2} \left| T_{a,b} \left[\frac{\partial}{\partial a} f_{a,b} \right] + \left[\frac{\partial}{\partial a} T_{a,b} \right] f_{a,b} \right| \leq \left| \frac{\partial}{\partial a} [T_{a,b} f_{a,b}] \right|.$$

Then from (14) and (16),

$$T_{a,b} f_{a,b} = \left(\frac{1 - \epsilon}{\epsilon} \right) \sqrt{2\pi} (\sigma^2 a + \lambda_t^2 b) \rho_{\nu_t} (\sigma^2 a + \lambda_t^2 b),$$

then using that $\frac{\partial}{\partial x} \rho_{\tau^2}(x) = -\frac{x}{\tau^2} \rho_{\tau^2}(x)$, we have

$$\begin{aligned} \left| \frac{\partial}{\partial a} [T_{a,b} f_{a,b}] \right| &= \left(\frac{1 - \epsilon}{\epsilon} \right) \sqrt{2\pi} \left| \sigma^2 \rho_{\nu_t} (\sigma^2 a + \lambda_t^2 b) \right. \\ &\quad \left. - \frac{\sigma^2 (\sigma^2 a + \lambda_t^2 b)^2}{\nu_t} \rho_{\nu_t} (\sigma^2 a + \lambda_t^2 b) \right| \\ &= \left(\frac{1 - \epsilon}{\epsilon} \right) \frac{\sqrt{2\pi} \sigma^2}{\nu_t} \rho_{\nu_t} (\sigma^2 a + \lambda_t^2 b) \\ &\quad \left| \nu_t - (\sigma^2 a + \lambda_t^2 b)^2 \right|. \end{aligned} \quad (18)$$

To upper bound the above, we use $\exp\{-x\} \leq \frac{1}{1+x}$ when $x \geq 0$, and so

$$\rho_{\tau^2}(x) = \frac{1}{\sqrt{2\pi\tau^2}} \exp\left\{-\frac{x^2}{2\tau^2}\right\} \leq \sqrt{\frac{2}{\pi}} \left(\frac{\tau}{2\tau^2 + x^2} \right).$$

Using this in (18), we find

$$\begin{aligned} \left| \frac{\partial}{\partial a} [T_{a,b} f_{a,b}] \right| &\leq \frac{2\sigma^2}{\sqrt{\nu_t}} \left(\frac{1 - \epsilon}{\epsilon} \right) \frac{|\nu_t - (\sigma^2 a + \lambda_t^2 b)^2|}{2\nu_t + (\sigma^2 a + \lambda_t^2 b)^2} \\ &\leq \frac{2\sigma^2}{\sqrt{\nu_t}} \left(\frac{1 - \epsilon}{\epsilon} \right) \leq \frac{2(1 - \epsilon)}{\sigma_w \epsilon}, \end{aligned} \quad (19)$$

where in the final inequality we use $\lambda_t \geq \sigma_w$ by (15), and

$$\begin{aligned} \frac{\sigma^2}{\sqrt{\nu_t}} &= \frac{\sigma}{\lambda_t \sqrt{\sigma^2 + \lambda_t^2 + \sigma^2 \lambda_t^2}} \\ &= \frac{1}{\lambda_t \sqrt{1 + \frac{\lambda_t^2}{\sigma^2} + \lambda_t^2}} \leq \frac{1}{\lambda_t}. \end{aligned} \quad (20)$$

Using the above in (17), we have

$$\left| \frac{\partial}{\partial a} \eta_t(a, b) \right| \leq 1 + \frac{2(1 - \epsilon)}{\sigma_w \epsilon}.$$

As in (17) we can show

$$\begin{aligned} \left| \frac{\partial}{\partial b} \eta_t(a, b) \right| &\leq \frac{(1 + 2T_{a,b})}{(1 + T_{a,b})^2} \left| \left[\frac{\partial}{\partial b} f_{a,b} \right] \right| \\ &\quad + \frac{1}{(1 + T_{a,b})^2} \left| T_{a,b} \left[\frac{\partial}{\partial b} f_{a,b} \right] + \left[\frac{\partial}{\partial b} T_{a,b} \right] f_{a,b} \right|, \end{aligned}$$

Then,

$$\frac{(1 + 2T_{a,b})}{(1 + T_{a,b})^2} \left| \frac{\partial}{\partial b} f_{a,b} \right| \leq 1,$$

and a bound as in (18) - (19) gives

$$\begin{aligned} \frac{1}{(1 + T_{a,b})^2} \left| T_{a,b} \left[\frac{\partial}{\partial b} f_{a,b} \right] + \left[\frac{\partial}{\partial b} T_{a,b} \right] f_{a,b} \right| &\leq \left| \frac{\partial}{\partial b} [T_{a,b} f_{a,b}] \right| \\ &\leq \frac{2\lambda_t^2}{\sqrt{\nu_t}} \left(\frac{1 - \epsilon}{\epsilon} \right) \frac{|\nu_t - (\sigma^2 a + \lambda_t^2 b)^2|}{2\nu_t + (\sigma^2 a + \lambda_t^2 b)^2} \\ &\leq \frac{2\lambda_t^2}{\sqrt{\nu_t}} \left(\frac{1 - \epsilon}{\epsilon} \right) \leq \frac{2(1 - \epsilon)}{\sigma \epsilon}. \end{aligned}$$

C. Numerical Examples

Finally, we provide numerical results to compare the empirical mean square error (MSE) performance of AMP-SI and the performance predicted by SE. Fig. 1 shows the MSE achieved by AMP-SI in the GG scenario and the SE prediction of its performance. In this example, the signal variance $\sigma_x^2 = 1$, the measurement noise variance $\sigma_w^2 = 0.01$, the variance of AWGN in SI $\sigma^2 = 0.04$. We averaged over 10 trials of a GG recovery problem for empirical results of AMP-SI. The comparison in Fig. 1(a), Fig. 1(b) and Fig. 1(c) given by three different signal length. For smaller n there is some gap between the empirical MSE and the SE prediction, as shown in Fig. 1 for $n = 100$, but the gap shrinks as n is increased. The results show the empirical MSE tracks the SE prediction nicely.

Fig. 2 shows the MSE achieved by AMP-SI in the BG scenario, and the SE prediction of its performance. We again averaged over 10 trials of a BG recovery problem for empirical results of AMP-SI. The signal length $n = 10000$, $m = 3000$, the measurement noise variance $\sigma_w^2 = 0.01$, and $\epsilon = 0.2$, where 20% of the entries in the signal are nonzero. We vary the variance of AWGN in SI from $\sigma^2 = 0.04$, $\sigma^2 = 0.25$, and $\sigma^2 = 1$. The results show that SE can predict the MSE achieved by AMP-SI at every iteration.

III. PROOF OF THEOREM II.1

Proof of The proof Theorem II.1 contains two steps. In the first step we use Berthier *et al.* [11, Theorem 14] and in the second step we make an appeal to the strong law of large numbers (SLLN). We remind the reader of the strong law:

Definition III.1. Strong Law of Large Numbers [15]: Let X_1, X_2, \dots be a sequence of i.i.d. random variables with finite mean μ . Then

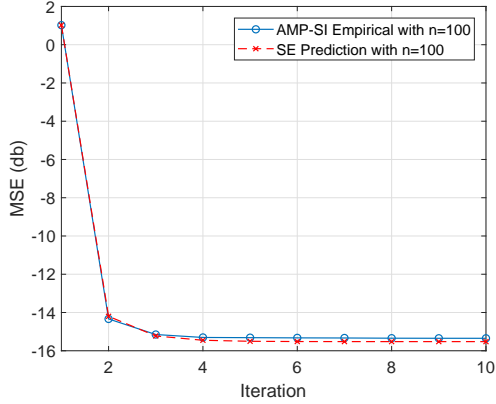
$$\Pr = \left(\lim_{n \rightarrow \infty} \frac{1}{n} (X_1 + X_2 + \dots + X_n) = \mu \right) = 1, \quad (21)$$

In words, the partial averages $\frac{1}{n} (X_1 + X_2 + \dots + X_n)$ converge almost surely to $\mu < \infty$.

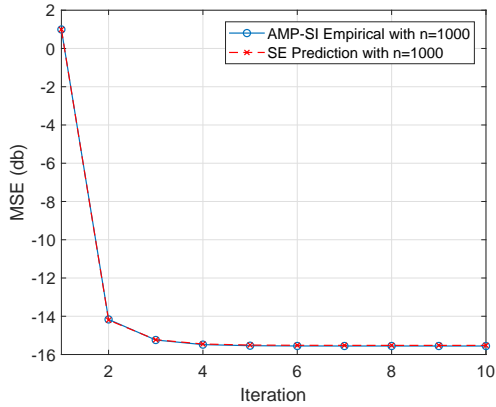
A. Step 1

We will make use of Berthier *et al.* [11, Theorem 14], restated here for convenience. Before proceeding we include a definition of *uniformly* pseudo-Lipschitz functions, that generalizes the ideal of pseudo-Lipschitz functions given in Definition II.1.

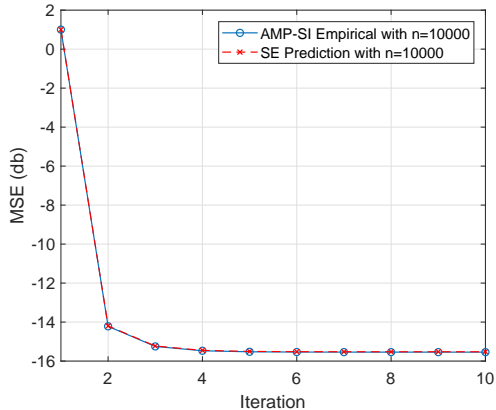
Definition III.2. Uniformly pseudo-Lipschitz functions [11]: A sequence (in n) of pseudo-Lipschitz functions $\{\phi_n\}_{n \in \mathbb{N}_{>0}}$



(a) n=100



(b) n=1000



(c) n=10000

Fig. 1: Empirical MSE performance of AMP-SI and SE prediction. (GG model, $\delta = 0.3$, $\sigma_x = 1$, $\sigma_w = 0.1$, and $\sigma = 0.2$.)

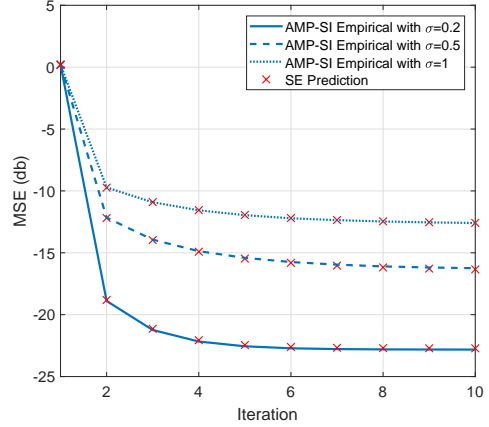


Fig. 2: Empirical MSE performance of AMP-SI and SE prediction. (BG model, $n = 10000$, $m = 3000$, $\epsilon = 0.2$, $\sigma_w = 0.1$.)

is called *uniformly pseudo-Lipschitz* of order k if, denoting by L_n is the pseudo-Lipschitz constant of order k of ϕ_n , we have $L_n < \infty$ for each n and $\limsup_{n \rightarrow \infty} L_n < \infty$.

Berthier *et al.* [11, Theorem 14] requires the following assumptions:

- (C1) The measurement matrix A has Gaussian entries with i.i.d. mean 0 and variance $1/m$.
- (C2) Define a sequence of denoisers $\tilde{\eta}_n^t : \mathbb{R}^n \rightarrow \mathbb{R}^n$ to be those that apply the denoiser η_t defined in (2) element-wise on vector input: $\tilde{\eta}_n^t(X) := \eta_t(X, \tilde{X})$. For each t , $\tilde{\eta}_n^t(\cdot)$ are uniformly Lipschitz. A function is *uniformly Lipschitz* in n if the Lipschitz constant does not depend on n .
- (C3) $\|x\|_2^2/n$ converges to a constant as $n \rightarrow \infty$.
- (C4) The limit $\sigma_w = \lim_{m \rightarrow \infty} \|w\|_2/\sqrt{m}$ is finite.
- (C5) For any iterations $s, t \in \mathbb{N}$ and for any 2×2 covariance matrix Σ , the following limits exist.

$$\lim_{n \rightarrow \infty} \frac{1}{n} \sum_{i=1}^n \mathbb{E}_Z [x_i \eta_t(x_i + Z_i, \tilde{x}_i)] < \infty,$$

$$\lim_{n \rightarrow \infty} \frac{1}{n} \sum_{i=1}^n \mathbb{E}_{Z, Z'} [\eta_t(x_i + Z_i, \tilde{x}_i) \eta_s(x_i + Z'_i, \tilde{x}_i)] < \infty,$$

where $(Z, Z') \sim \mathcal{N}(0, \Sigma \otimes \mathbb{I}_n)$, with \otimes denoting the tensor product and \mathbb{I}_n the identity matrix.

Theorem III.1. *Under the assumptions (C1) – (C5), for any sequences of uniformly pseudo-Lipschitz functions $\phi_n : \mathbb{R}^m \times \mathbb{R}^m \rightarrow \mathbb{R}$ and $\psi_n : \mathbb{R}^n \times \mathbb{R}^n \rightarrow \mathbb{R}$,*

$$\lim_m \left(\phi_m(r^t, w) - \mathbb{E}_{Z_1} \left[\phi_m(w + \sqrt{\lambda_t^2 - \sigma_w^2} Z_1, w) \right] \right) \stackrel{p}{=} 0,$$

$$\lim_n \left(\psi_n(x^t + A^T r^t, x) - \mathbb{E}_{Z_2} [\psi_n(x + \lambda_t Z_2, x)] \right) \stackrel{p}{=} 0,$$

where $Z_1 \sim \mathcal{N}(0, \mathbb{I}_m)$, $Z_2 \sim \mathcal{N}(0, \mathbb{I}_n)$, x^t and r^t are defined in the AMP-SI recursion (3)-(4), and λ_t in the SE (5).

Now we demonstrate that our assumptions **(A1)** – **(A4)** stated in Section II are enough to satisfy the assumptions **(C1)** – **(C6)** needed to apply Theorem III.1.

Assumptions **(A1)** and **(C1)** are identical. We will show that **(C2)** follows from **(A4)**, **(C4)** follows from **(A2)**, and **(C3)** follows from **(A3)**. Finally we show **(C5)** and **(C6)** follow from **(A3)** and **(A4)**.

First consider assumption **(C2)**. The non-separable denoiser $\tilde{\eta}_n^t(X) = \eta_t(X, \tilde{X})$ applies the AMP-SI denoiser defined in (2) entrywise to its vector inputs. From **(A4)**, $\{\eta_t(\cdot, \cdot)\}_{t \geq 0}$ are Lipschitz continuous. Thus, for length- n vectors x_1, x_2 , and fixed SI \tilde{x} ,

$$\begin{aligned} \|\tilde{\eta}_n^t(x_1) - \tilde{\eta}_n^t(x_2)\|^2 &= \sum_{i=1}^n (\eta_t([x_1]_i, \tilde{x}_i) - \eta_t([x_2]_i, \tilde{x}_i))^2 \\ &\leq \sum_{i=1}^n L^2([x_1]_i - [x_2]_i)^2 = L^2 \|x_1 - x_2\|^2, \end{aligned}$$

and so

$$\|\tilde{\eta}_n^t(x_1) - \tilde{\eta}_n^t(x_2)\| \leq L \|x_1 - x_2\|.$$

The Lipschitz constant does not depend on n , so $\tilde{\eta}_n^t(\cdot)$ is uniformly Lipschitz.

Now consider assumption **(C4)**. From **(A2)**, the measurement noise w in (1) has i.i.d. entries with zero-mean and finite $\mathbb{E}[|W|^k]$. Then applying Definition III.1,

$$\lim_{m \rightarrow \infty} \frac{\|w\|_2^2}{m} = \lim_{m \rightarrow \infty} \frac{1}{m} \sum_{i=1}^m w_i^2 = \sigma_w^2 < \infty,$$

where we have used that $\sigma_w^2 < \infty$ follows from $\mathbb{E}[|W|^k] < \infty$ for $k \geq 2$. The proof of **(C3)** similarly follows using the SLLN and the finiteness of $\mathbb{E}[|X|^k]$ given in assumption **(A3)**.

We now show that **(C5)** is met. Recall $Z \sim \mathcal{N}(0, \sigma_z^2 \mathbb{I}_n)$. Define $y_i := x_i \mathbb{E}_Z [\eta_t(x_i + Z_i, \tilde{x}_i)]$ for $i = 1, 2, \dots, n$. By assumption **(A3)**, the signal and side information (X, \tilde{X}) are sampled i.i.d. from the joint density $f(X, \tilde{X})$. It follows that y_1, y_2, \dots, y_n are also i.i.d., so by Definition III.1 if $\mathbb{E}[X \eta_t(X + Z, \tilde{X})] < \infty$ where $Z \sim \mathcal{N}(0, \sigma_z^2)$ independent of $(X, \tilde{X}) \sim f(X, \tilde{X})$, then

$$\lim_{n \rightarrow \infty} \frac{1}{n} \sum_{i=1}^n x_i \mathbb{E}_Z [\eta_t(x_i + Z_i, \tilde{x}_i)] = \mathbb{E}[X \eta_t(X + Z, \tilde{X})],$$

We will now show that $\mathbb{E}[X \eta_t(X + Z, \tilde{X})] < \infty$.

First note that **(A4)** assumes $\eta_t(\cdot, \cdot)$ is Lipschitz, meaning for scalars a_1, a_2, b_1, b_2 and some constant $L > 0$,

$$\begin{aligned} |\eta_t(a_1, b_1) - \eta_t(a_2, b_2)| &\leq L(|a_1 - a_2| + |b_1 - b_2|) \\ &\leq L|a_1 - a_2| + L|b_1 - b_2|. \end{aligned}$$

Therefore letting $a_2 = b_2 = 0$ we have

$$|\eta_t(a_1, b_1) - \eta_t(0, 0)| \leq |\eta_t(a_1, b_1) - \eta_t(0, 0)| \leq L|a_1| + L|b_1|,$$

giving the follows upper bound for constant $L' > 0$,

$$|\eta_t(a_1, b_1)| \leq L'(1 + |a_1| + |b_1|). \quad (22)$$

Now using (22) and the triangle inequality,

$$\begin{aligned} \mathbb{E}[X \eta_t(X + Z, \tilde{X})] &\leq L' \mathbb{E}[|X|(1 + |X + Z| + |\tilde{X}|)] \\ &\leq L' (\mathbb{E}[|X|] + \mathbb{E}[X^2] + \mathbb{E}[|X| \mathbb{E}[|Z|] + \mathbb{E}[|X \tilde{X}|]). \end{aligned} \quad (23)$$

Finally, by assumption **(A3)** we have that $\mathbb{E}[|X|^k]$, $\mathbb{E}[|\tilde{X}|^k]$ and $\mathbb{E}[|X \tilde{X}|]$ are all finite. Then noting that for any random variable, Y , we have $|Y|^r \leq 1 + |Y|^k$ for $1 \leq r \leq k$, meaning $\mathbb{E}[|Y|^r] < 1 + \mathbb{E}[|Y|^k]$ the boundedness of $\mathbb{E}[X \eta_t(X + Z, \tilde{X})]$ follows from (23) with assumption **(A3)**.

The proof of **(C6)** follows similarly to the proof of **(C5)**. Recall $(Z, Z') \sim N(0, \Sigma \otimes \mathbb{I}_n)$. Define $y_i := \mathbb{E}_{Z, Z'} [\eta_t(x_i + Z_i, \tilde{x}_i) \eta_s(x_i + Z'_i, \tilde{x}_i)]$ for $i = 1, 2, \dots, n$. By assumption **(A3)**, the signal and side information (X, \tilde{X}) are sampled i.i.d. from the joint density $f(X, \tilde{X})$. It follows that y_1, y_2, \dots, y_n are also i.i.d., so by Definition III.1 if $\mathbb{E}[\eta_t(X + Z, \tilde{X}) \eta_s(X + Z', \tilde{X})] < \infty$ where $Z \sim \mathcal{N}(0, \sigma_z^2)$ and $Z' \sim \mathcal{N}(0, \sigma_{z'}^2)$, independent of $(X, \tilde{X}) \sim f(X, \tilde{X})$, then

$$\begin{aligned} \lim_{n \rightarrow \infty} \frac{1}{n} \sum_{i=1}^n \mathbb{E}_{Z, Z'} [\eta_t(x_i + Z_i, \tilde{x}_i) \eta_s(x_i + Z'_i, \tilde{x}_i)] \\ = \mathbb{E}[\eta_t(X + Z, \tilde{X}) \eta_s(X + Z', \tilde{X})]. \end{aligned}$$

We will now show that $\mathbb{E}[\eta_t(X + Z, \tilde{X}) \eta_s(X + Z', \tilde{X})] < \infty$. Using the bound (22),

$$\begin{aligned} \mathbb{E}[\eta_t(X + Z, \tilde{X}) \eta_s(X + Z', \tilde{X})] \\ \leq \mathbb{E}[|\eta_t(X + Z, \tilde{X})| |\eta_s(X + Z', \tilde{X})|] \\ \leq L'^2 \mathbb{E}[(1 + |X + Z| + |\tilde{X}|)(1 + |X + Z'| + |\tilde{X}|)]. \end{aligned}$$

Then using the triangle inequality,

$$\begin{aligned} \mathbb{E} \left[(1 + |X + Z| + |\tilde{X}|)(1 + |X + Z'| + |\tilde{X}|) \right] \\ \leq \mathbb{E} \left[(1 + |X| + |Z| + |\tilde{X}|)(1 + |X| + |Z'| + |\tilde{X}|) \right] \\ = 1 + 2\mathbb{E}[|X|] + 2\mathbb{E}[|\tilde{X}|] + 2\mathbb{E}[|X||\tilde{X}|] + \mathbb{E}[X^2] + \mathbb{E}[\tilde{X}^2] \\ + \mathbb{E}[|X||Z'|] + \mathbb{E}[|X||Z|] + \mathbb{E}[|\tilde{X}||Z'|] + \mathbb{E}[|\tilde{X}||Z|] \\ + \mathbb{E}[|Z|] + \mathbb{E}[|Z'|] + \mathbb{E}[|Z||Z'|] \\ = 1 + 2\mathbb{E}[|X|] + 2\mathbb{E}[|\tilde{X}|] + 2\mathbb{E}[|X\tilde{X}|] + \mathbb{E}[X^2] + \mathbb{E}[\tilde{X}^2] \\ + \mathbb{E}[|Z'|](1 + \mathbb{E}[|X|] + \mathbb{E}[|\tilde{X}|]) + \mathbb{E}[|Z|](1 \\ + \mathbb{E}[|X|] + \mathbb{E}[|\tilde{X}|]) + \mathbb{E}[|ZZ'|]. \end{aligned} \quad (24)$$

Finally we apply Theorem III.1 to the sequences of uniformly pseudo-Lipschitz functions $\phi_m : \mathbb{R}^m \times \mathbb{R}^m \rightarrow \mathbb{R}$ and $\psi_n : \mathbb{R}^n \times \mathbb{R}^n \rightarrow \mathbb{R}$ defined as follows: for vectors $a, b \in \mathbb{R}^m$ and $x, y, \tilde{x} \in \mathbb{R}^n$,

$$\phi_m(a, b) := \frac{1}{m} \sum_{i=1}^m \phi(a_i, b_i), \quad (25)$$

$$\text{and } \psi_n(x, y) := \frac{1}{n} \sum_{i=1}^n \psi(x_i, y_i, \tilde{x}_i),$$

where ϕ and ψ are the pseudo-Lipschitz functions defined in Theorem II.1. This then gives the result

$$\begin{aligned} & \lim_n \frac{1}{m} \sum_{i=1}^m \phi(r_i^t, w_i) \\ & \stackrel{p}{=} \lim_n \frac{1}{m} \sum_{i=1}^m \mathbb{E}_{Z_1} \left[\phi(w_i + \sqrt{\lambda_t^2 - \sigma_w^2} Z_1, w_i) \right], \end{aligned} \quad (26)$$

and

$$\begin{aligned} & \lim_n \frac{1}{n} \sum_{i=1}^n \psi(x_i^t + [A^T r^t]_i, x_i, \tilde{x}_i) \\ & \stackrel{p}{=} \lim_n \frac{1}{n} \sum_{i=1}^n \mathbb{E}_{Z_2} [\psi(x_i + \lambda_t Z_2, x_i, \tilde{x}_i)]. \end{aligned} \quad (27)$$

As a final step, we show that the functions defined in (25) are uniformly pseudo-Lipschitz as needed to apply Theorem III.1. Using that $\phi : \mathbb{R}^2 \rightarrow \mathbb{R}$ is pseudo-Lipschitz of order k , meaning for vectors $a_1, a_2, b_1, b_2 \in \mathbb{R}^m$, any index $i = 1, 2, \dots, m$

$$\begin{aligned} \left| \phi(a_i, \tilde{a}_i) - \phi(b_i, \tilde{b}_i) \right| & \leq L \left(1 + \frac{1}{\sqrt{2}} \left\| (a_i, \tilde{a}_i) \right\|^{k-1} \right. \\ & \quad \left. + \frac{1}{\sqrt{2}} \left\| (b_i, \tilde{b}_i) \right\|^{k-1} \right) \frac{1}{\sqrt{2}} \left\| (a_i, \tilde{a}_i) - (b_i, \tilde{b}_i) \right\|, \end{aligned}$$

where $L > 0$ is some constant. Then using the above,

$$\begin{aligned} \left| \phi_m(a, \tilde{a}) - \phi_m(b, \tilde{b}) \right| & \leq \frac{1}{m} \sum_{i=1}^m \left| \phi(a_i, \tilde{a}_i) - \phi(b_i, \tilde{b}_i) \right| \\ & \leq \frac{L}{m} \sum_{i=1}^m \left(1 + \frac{1}{\sqrt{2}} \left\| (a_i, \tilde{a}_i) \right\|^{k-1} + \frac{1}{\sqrt{2}} \left\| (b_i, \tilde{b}_i) \right\|^{k-1} \right) \\ & \quad \times \frac{1}{\sqrt{2}} \left\| (a_i, \tilde{a}_i) - (b_i, \tilde{b}_i) \right\| \\ & \leq \frac{L}{\sqrt{2m}} \left(\sqrt{2m} + \sqrt{\sum_{i=1}^m \left\| (a_i, \tilde{a}_i) \right\|^{2(k-1)}} + \sqrt{\sum_{i=1}^m \left\| (b_i, \tilde{b}_i) \right\|^{2(k-1)}} \right) \\ & \quad \times \sqrt{\sum_{i=1}^m \left\| (a_i, \tilde{a}_i) - (b_i, \tilde{b}_i) \right\|^2} \end{aligned} \quad (28)$$

where the final step follows by Cauchy-Schwarz. First note

$$\begin{aligned} & \sum_{i=1}^m \left\| (a_i, \tilde{a}_i) - (b_i, \tilde{b}_i) \right\|^2 \\ & = \sum_{i=1}^m \left((a_i - b_i)^2 + (\tilde{a}_i - \tilde{b}_i)^2 \right) = \left\| (a, \tilde{a}) - (b, \tilde{b}) \right\|^2 \end{aligned} \quad (29)$$

where $\left\| (a, \tilde{a}) - (b, \tilde{b}) \right\|^2$ considers the object $(a, \tilde{a}) \in \mathbb{R}^m \times \mathbb{R}^m$ to be a single length- $2m$ vector, so

$$\left\| (a, \tilde{a}) - (b, \tilde{b}) \right\|^2 = \|a - b\|^2 + \|\tilde{a} - \tilde{b}\|^2.$$

Next, note that for vectors $v, w \in \mathbb{R}^m$ we have $\sum_{i=1}^m (|v_i| + |w_i|)^k \leq (\sum_{i=1}^m |v_i| + \sum_{i=1}^m |w_i|)^k$. Then,

$$\begin{aligned} & \sum_{i=1}^m \left\| (a_i, \tilde{a}_i) \right\|^{2(k-1)} = \sum_{i=1}^m \left((a_i)^2 + (\tilde{a}_i)^2 \right)^{k-1} \\ & \leq \left(\sum_{i=1}^m (a_i)^2 + \sum_{i=1}^m (\tilde{a}_i)^2 \right)^{(k-1)} \leq (\|a\|^2 + \|\tilde{a}\|^2)^{k-1} \quad (30) \\ & = \left\| (a, \tilde{a}) \right\|^{2(k-1)}, \end{aligned}$$

where the final step follows since by $\left\| (a, \tilde{a}) \right\|^{k-1}$ we mean to think of the object $(a, \tilde{a}) \in \mathbb{R}^m \times \mathbb{R}^m$ as single length- $2m$ vector, so

$$\begin{aligned} \left\| (a, \tilde{a}) \right\|^{2(k-1)} & = \left(\sum_{i=1}^m (a_i)^2 + \sum_{i=1}^m (\tilde{a}_i)^2 \right)^{k-1} \\ & = \left(\|a\|^2 + \|\tilde{a}\|^2 \right)^{k-1} \end{aligned} \quad (31)$$

Now putting (29) and (30) into (28) we have the desired result,

$$\begin{aligned} & \left| \phi_m(a, \tilde{a}) - \phi_m(b, \tilde{b}) \right| \\ & \leq L \left(1 + \frac{1}{\sqrt{2m}} \left\| (a, \tilde{a}) \right\|^{k-1} + \frac{1}{\sqrt{2m}} \left\| (b, \tilde{b}) \right\|^{k-1} \right) \\ & \quad \frac{1}{\sqrt{2m}} \left\| (a, \tilde{a}) - (b, \tilde{b}) \right\|. \end{aligned} \quad (32)$$

B. Step 2

Now consider the step 1 result (26), our final goal is do demonstrate

$$\begin{aligned} & \lim_m \frac{1}{m} \sum_{i=1}^m \mathbb{E}_{Z_1} \left[\phi(w_i + \sqrt{\lambda_t^2 - \sigma_w^2} Z_1, w_i) \right] \\ & \stackrel{a.s.}{=} \mathbb{E} \left[\phi(W + \sqrt{\lambda_t^2 - \sigma_w^2} Z_1, W) \right], \end{aligned}$$

$$\lim_n \frac{1}{n} \sum_{i=1}^n \mathbb{E}_{Z_2} [\psi(x_i + \lambda_t Z_2, x_i, \tilde{x}_i)] \stackrel{a.s.}{=} \mathbb{E} [\psi(X + \lambda_t Z_2, X, \tilde{X})].$$

The result follows by the SLLN (Definition III.1) so long as $\mathbb{E}[\phi(W + \sqrt{\lambda_t^2 - \sigma_w^2} Z_1, W)]$ and $\mathbb{E}[\psi(X + \lambda_t Z_2, X, \tilde{X})]$ are both finite. Recall, if $\phi : \mathbb{R}^n \rightarrow \mathbb{R}$, is a pseudo-Lipschitz function of order k , then there is a constant $L' > 0$ such that for all $x \in \mathbb{R}^n : |\phi(x)| \leq L' (1 + \|x\|^k)$ [9]. Using this,

$$\begin{aligned} & \left| \phi(W + \sqrt{\lambda_t^2 - \sigma_w^2} Z_1, W) \right| \\ & \leq L'_1 \left(1 + \left\| (W + \sqrt{\lambda_t^2 - \sigma_w^2} Z_1, W) \right\|^k / \sqrt{2} \right) \quad (33) \\ & \leq L'_1 \left(1 + \frac{6^{k/2}}{2\sqrt{2}} |W|^k + \frac{4^{k/2}}{2\sqrt{2}} (\lambda_t^2 - \sigma_w^2)^{k/2} |Z_1|^k \right), \end{aligned}$$

where we have used that

$$\begin{aligned} & \left\| \left(W + \sqrt{\lambda_t^2 - \sigma_w^2} Z_1, W \right) \right\|^k \\ &= \left(\left(W + \sqrt{\lambda_t^2 - \sigma_w^2} Z_1 \right)^2 + W^2 \right)^{\frac{k}{2}} \\ &\leq (3W^2 + 2(\lambda_t^2 - \sigma_w^2)Z_1^2)^{\frac{k}{2}} \\ &\leq \frac{6^{\frac{k}{2}}}{2} |W|^k + 2^{k-1} (\lambda_t^2 - \sigma_w^2)^{\frac{k}{2}} |Z_1|^k. \end{aligned}$$

Then, using (33), and the boundedness of $\mathbb{E}[|W|^k]$ by (A2),

$$\begin{aligned} & \mathbb{E} \left| \phi(W + \sqrt{\lambda_t^2 - \sigma_w^2} Z_1, W) \right| \\ &\leq L'_1 \left(1 + \frac{6^{\frac{k}{2}}}{2} \mathbb{E}[|W|^k] + \frac{4^{\frac{k}{2}}}{2} (\lambda_t^2 - \sigma_w^2)^{\frac{k}{2}} \mathbb{E}[|Z_1|^k] \right) < \infty. \end{aligned}$$

Similarly, we have the upper bound,

$$\begin{aligned} & \left| \psi(X + \lambda_t Z_2, X, \tilde{X}) \right| \leq L'_2 \left(1 + \left\| (X + \lambda_t Z_2, X, \tilde{X}) \right\|^k / \sqrt{3} \right) \\ &\leq L'_2 \left(1 + \frac{3^{k-1}}{\sqrt{3}} |X|^k + \frac{6^{k/2}}{3\sqrt{3}} \lambda_t^k |Z_2|^k + \frac{3^{k/2}}{3\sqrt{3}} |\tilde{X}|^k \right), \end{aligned} \quad (34)$$

where we have used that

$$\begin{aligned} \left\| (X + \lambda_t Z_2, X, \tilde{X}) \right\|^k &= \left((X + \lambda_t Z_2)^2 + X^2 + \tilde{X}^2 \right)^{k/2} \\ &\leq \left(3X^2 + 2\lambda_t^2 Z_2^2 + \tilde{X}^2 \right)^{k/2} \\ &\leq 3^{k-1} |X|^k + \frac{6^{k/2}}{3} \lambda_t^k |Z_2|^k + \frac{3^{k/2}}{3} |\tilde{X}|^k. \end{aligned}$$

Therefore, using (34), and the boundedness of $\mathbb{E}[|X|^k]$ and $\mathbb{E}[|\tilde{X}|^k]$ assumed in (A3),

$$\begin{aligned} & \mathbb{E}[\psi(X + \lambda_t Z_2, X, \tilde{X})] \\ &\leq L'_2 \left(1 + 3^{k-1} \mathbb{E}[|X|^k] + \frac{6^{k/2}}{3} \lambda_t^k \mathbb{E}[|Z_2|^k] + \frac{1}{3} 3^{k/2} \mathbb{E}[|\tilde{X}|^k] \right) < \infty. \end{aligned}$$

ACKNOWLEDGMENT

We thank You (Joe) Zhou for insightful conversations and valuable advice. In addition, Liu and Baron acknowledge support from NSF EECS #1611112.

REFERENCES

- [1] D. L. Donoho, A. Maleki, and A. Montanari, "Message passing algorithms for compressed sensing," *Proc. Nat. Academy Sci.*, vol. 106, no. 45, pp. 18914–18919, Nov. 2009.
- [2] H. Arguello and G. Arce, "Code aperture optimization for spectrally agile compressive imaging," *J. Opt. Soc. Am.*, vol. 28, no. 11, pp. 2400–2413, Nov. 2011.
- [3] T. Hastie, R. Tibshirani, and J. H. Friedman, *The Elements of Statistical Learning*. Springer, Aug. 2001.
- [4] S. Rangan, "Generalized approximate message passing for estimation with random linear mixing," *Arxiv preprint arXiv:1010.5141*, Oct. 2010.
- [5] T. M. Cover and J. A. Thomas, *Elements of Information Theory*. New York, NY, USA: Wiley-Interscience, 2006.
- [6] D. Baron, A. Ma, D. Needell, C. Rush, and T. Woolf, "Conditional approximate message passing with side information," in *Proc. IEEE Asilomar Conf. Signals, Syst. Comput.*, 2017.

- [7] A. Ma, Y. Zhou, C. Rush, D. Baron, and D. Needell, "An approximate message passing framework for side information," *arXiv:1807.04839*, Jul. 2018.
- [8] A. Saleh and R. Valenzuela, "A statistical model for indoor multipath propagation," *IEEE J. Select. Areas Commun.*, vol. 5, no. 2, pp. 128–137, Feb. 1987.
- [9] M. Bayati and A. Montanari, "The dynamics of message passing on dense graphs, with applications to compressed sensing," *IEEE Trans. Inf. Theory*, vol. 57, no. 2, pp. 764–785, Feb. 2011.
- [10] C. Rush and R. Venkataramanan, "Finite sample analysis of approximate message passing algorithms," *IEEE Trans. Inf. Theory*, vol. 64, no. 11, pp. 7264–7286, Nov. 2018.
- [11] R. Berthier, A. Montanari, and P. M. Nguyen, "State evolution for approximate message passing with non-separable functions," *arXiv:1708.03950*, Aug. 2017.
- [12] X. Wang and J. Liang, "Approximate message passing-based compressed sensing reconstruction with generalized elastic net prior," *Signal Process. Image*, vol. 37, pp. 19–33, Sept. 2015.
- [13] J. Ziniel and P. Schniter, "Dynamic compressive sensing of time-varying signals via approximate message passing," *IEEE Trans. Signal Process.*, vol. 61, no. 21, pp. 5270–5284, Nov. 2013.
- [14] A. Manoel, F. Krzakala, E. W. Tramel, and L. Zdeborová, "Streaming bayesian inference: theoretical limits and mini-batch approximate message-passing," in *Communication, Control, and Computing (Allerton), 2017 55th Annual Allerton Conference on*. IEEE, 2017, pp. 1048–1055.
- [15] J. S. Rosenthal, *A First Look at Rigorous Probability Theory*, 2nd ed. World Scientific Publishing Co. Pte. Ltd., 2006.